

RESEARCH ARTICLE

Enzymatic post-crosslinking of printed hydrogels of methacrylated gelatin and tyramine-conjugated 8-arm poly(ethylene glycol) to prepare interpenetrating 3D network structures

Jia Liang^{1,2}, Zhule Wang³, Andreas A. Poot², Dirk W. Grijpma², Piet J. Dijkstra², Rong Wang^{2,3*}

¹Department of Neurosurgery, Stroke Center, Henan Provincial People's Hospital, 450003, Henan, China

²Department of Biomaterials Science and Technology, University of Twente, Drienerlolaan 5, 7522 NB Enschede, The Netherlands

³Department of Dentistry-Regenerative Biomaterials, Radboud University Medical Center, Philips van Leydenlaan 25, 6525 EX Nijmegen, The Netherlands

(This article belongs to the *Special Issue: Additive Manufacturing of Functional Biomaterials*)

Abstract

Methacrylated gelatin (GelMA) has been intensively studied as a 3D printable scaffold material in tissue regeneration fields, which can be attributed to its well-known biological functions. However, the long-term stability of photo-crosslinked GelMA scaffolds is hampered by a combination of its fast degradation in the presence of collagenase and the loss of physical crosslinks at higher temperatures. To increase the longer-term shape stability of printed scaffolds, a mixture of GelMA and tyramine-conjugated 8-arm PEG (8PEGTA) was used to create filaments composed of an interpenetrating network (IPN). Photo-crosslinking during filament deposition of the GelMA and subsequent enzymatic crosslinking of the 8PEGTA were applied to the printed 3D scaffolds. Although both crosslinking mechanisms are radical based, they operate without interference of each other. Rheological data of bulk hydrogels showed that the IPN was an elastic hydrogel, having a storage modulus of 6 kPa, independent of temperature in the range of 10 – 40°C. Tensile and compression moduli were 110 kPa and 80 kPa, respectively. On enzymatic degradation in the presence of collagenase, the gelatin content of the IPN fully degraded in 7 days, leaving a stable secondary crosslinked 8PEGTA network. Using a BioMaker bioprinter, hydrogels without and with human osteosarcoma cells (hMG-63) were printed. On culturing for 21 days, hMG-63 in the GelMA/8PEGTA IPN showed a high cell viability (>90%). Thus, the presence of the photoinitiator, incubation with H₂O₂, and mechanical forces during printing did not hamper cell viability. This study shows that the GelMA/8PEGTA ink is a good candidate to generate cell-laden bioinks for extrusion-based printing of constructs for tissue engineering applications.

Keywords: GelMA; 8-arm PEG; Photo-crosslinking; Enzymatic crosslinking; Bioprinting

***Corresponding author:**

Rong Wang
(rong.wang@radboudumc.nl)

Citation: Liang J, Wang Z, Poot AA, 2023, Enzymatic post-crosslinking of printed hydrogels of methacrylated gelatin and tyramine-conjugated 8-arm poly(ethylene glycol) to prepare interpenetrating 3D network structures. *Int J Bioprint*, 9(5): 750.
<https://doi.org/10.18063/ijb.750>

Received: September 13, 2022

Accepted: November 7, 2022

Published Online: May 11, 2023

Copyright: © 2023 Author(s). This is an Open Access article distributed under the terms of the Creative Commons Attribution License, permitting distribution, and reproduction in any medium, provided the original work is properly cited.

Publisher's Note: Whioce Publishing remains neutral with regard to jurisdictional claims in published maps and institutional affiliations.

1. Introduction

Hydrogels, water-swollen networks of synthetic or natural polymers, have shown large potential in biomedical and pharmaceutical applications during the past decades^[1]. Due to their generally viscoelastic properties and high water content, they resemble the properties of the natural extracellular matrix. In many studies, it has been shown that hydrogels provide a biologically compatible environment for cells^[2]. To bioengineer 3D-printed hydrogel scaffolds for tissue regeneration, the chemical, physical, mechanical, and biological properties of the materials must be accounted for Ouyang *et al.*,^[3] Annabi *et al.*,^[4] Hoch *et al.*^[5]. Viscosity and cytocompatibility of materials, crosslinking kinetics to stabilize scaffolds, and degradation rate of (cell-laden) constructs all must be considered in the preparation of printed scaffolds^[6,7].

Choices for physical and covalent crosslinking of biologically relevant natural and synthetic polymers such as gelatin, hyaluronic acid, and aliphatic polyesters, respectively, are key issues in the 3D printing of hydrogels^[8]. One of the most applied materials for extrusion-based bioprinting is methacrylated gelatin (GelMA)^[6,9,10]. Like gelatin, GelMA retains a structural rearrangement in triple helical content with temperature. Below room temperature, physical crosslinks are formed and a stable printed structure can be deposited with unparalleled spatial and temporal control. The structure is then further stabilized by covalent crosslinking of the vinyl groups through photo-polymerization^[11]. Furthermore, GelMA with different degrees of functionalization can be reproducibly prepared^[12]. Even at high degrees of substitution, cell adhesion through the presence of RGD and other sequences like DGEA retains this material highly suitable for the construction of networks applicable for tissue regeneration purposes^[13]. However, a disadvantage of photo-crosslinked GelMA is the rapid enzymatic degradation by collagenase, generally within hours, making this material less suitable for regeneration of most tissues^[14].

Poly(ethylene glycol)s (PEGs), as non-toxic and non-immunogenic polymers, are highly suitable materials to be applied in the preparation of hydrogels although they lack cell recognition and cell adhesion^[15,16]. Compared to linear PEGs, multi-arm PEGs provide a higher molar of end groups, which have shown to largely improve the mechanical properties of crosslinked hydrogels^[17]. However, these types of polymers have a low viscosity (10 – 100 cm³/g) and do not retain shape stability on extrusion-based printing^[18-20]. In the work by Shah *et al.*, the homodifunctionalized PEGs were employed as crosslinking agents in preparing bioinks that capable of extrudable. The end groups of PEGs can form lightly crosslinks with different nature polymers, such

as gelatin and fibronectin with versatility and tunability. By adjusting the length of PEG chain segments and the number of branched chains, 3D printing gels with different mechanical strengths can be obtained^[21]. In our previous work, hybrid hydrogels made from 50% PEG-dMA: 50% GelMA have been reported. It is known that the toughness of this hybrid hydrogel was 2.5 times higher than that of hydrogels prepared from either PEG-dMA or GelMA with the same solid content^[22].

A strategy of combining the advantages of these widely studied biomaterials may well serve the design of bioink candidates for fabrication of scaffolds and integrate specific properties such as bio-adhesion and cell recognition, improved mechanical properties, and prolonged degradation times from days to weeks^[12,23]. In the design of such hybrid hydrogels^[24,25], the use of two crosslinking mechanisms can be employed when macromers have different functionalities. Such an approach provides an interpenetrating network (IPN) in which a second polymer network is placed within a crosslinked hydrogel primary network^[26].

Most IPNs studied for use in biofabrication are based on the combination of GelMA and alginate through photo-crosslinking and Ca²⁺ addition^[27-31]. Concentrations applied are generally in the range of 4 – 10 wt% for GelMA and 1 – 6 wt% for the alginate. Mechanical properties of these IPNs were either determined by rheological measurements, giving storage moduli ranging from 5 to 10 kPa, or compression tests, giving moduli ranging from 40 to 140 kPa. The crosslinking with calcium ions of a pectin grafted with poly(ϵ -caprolactone), and subsequent photo-crosslinking of GelMA provided IPN hydrogels with high compressive moduli up to 1 MPa depending on composition^[27,32]. GelMA was also combined with the fibrous protein collagen or silk fibroin^[33,34]. In the former case, IPN formation was performed by first collagen fiber formation at 37°C followed by photo-crosslinking of the GelMA. In the latter case, the mixture of GelMA and silk fibroin was first photo-crosslinked followed by treatment with methanol to induce silk fibroin β -sheet formation. Using GelMA and gellan gum methacrylate, an IPN with a compressive failure stress of up to 6.9 MPa could be prepared. The double network was formed by creating a gellan gum methacrylate network by photo-crosslinking. GelMA was diffused into this network and subsequently photo-crosslinked to give an IPN^[35].

To deliver an adequate 3D printable bioink candidate based on GelMA that can be post-stabilized, we designed a novel concept using a mixture of GelMA and an 8-arm PEG tyramine conjugate (8PEGTA). The GelMA provides constructs through physical and photo-crosslinking on printing. Enzymatic post-crosslinking of the 8PEGTA

component in the filaments, using horseradish peroxidase (HRP) as an enzymatic catalyst, provides an IPN composed of two chemically crosslinked networks. Such an IPN may improve the mechanical and degradation properties of GelMA constructs and retaining viability toward encapsulated cells. Photo-polymerization of GelMA during printing is a well-known method to stabilize GelMA-based printed scaffolds. HRP is a highly effective enzyme in the crosslinking of phenolated conjugates of synthetic and natural polymers such as poly(glutamic acid)^[36], gelatin^[37], dextran, and hyaluronic acid in the presence of very low concentrations of hydrogen peroxide^[38,39]. Although HRP was shown to catalyze the polymerization of, *for example*, acrylates and acrylamides, this requires a mediator like acetyl acetone to generate the necessary radicals to initiate polymerization^[40]. The absence of such a mediator may thus well be a basis for independent crosslinking of GelMA and phenols by consecutive photo-polymerization and enzymatic crosslinking, respectively. The mechanical and degradation properties of this IPN were compared to those of the GelMA single component network by rheological measurements and enzymatic degradation tests. Finally, the morphology and viability of human osteosarcoma cells (MG-63) after 3D printing of a cell-laden GelMA/8PEGTA bioink were investigated.

2. Materials and methods

2.1. Materials

GelMA with 90% of free amine groups substituted by methacrylate groups was synthesized as previously reported^[20]. The 8-arm PEG (8PEG, hexaglycerol core, $M_w = 20,000$ g/mol) was acquired from Jenkem Technology (Allen, Texas, USA), and freeze-dried overnight before use. p-Nitrophenyl chloroformate (PNC), tyramine (TA), lithium phenyl-2,4,6-trimethylbenzoylphosphinate (LAP), hydrogen peroxide (H_2O_2 , 30 wt% in H_2O), horseradish peroxidase (HRP) (253 U/mg), hexamethyldisilazane (HMDS), sodium azide, phosphate-buffered saline (PBS), and N, N-dimethylformamide (DMF) were obtained from Sigma-Aldrich. Collagenase (Type I, 260 U/mg) was obtained from Thermo Fisher Scientific. Diethyl ether, dichloromethane, and ethanol were purchased from VWR Chemicals. Dulbecco's PBS (DPBS, Gibco), α -MEM (A22571, Gibco), fetal bovine serum (FBS, Lonza, Basel, Switzerland), GlutaMAX, trypsin/EDTA, and penicillin/streptomycin (G418) were obtained from Gibco. Live/dead cell viability kit was purchased from Invitrogen Molecular Probes (L3224, Thermo Fisher Scientific, Eugene, USA).

2.2. 8-arm PEG-tyramine-conjugated synthesis

8PEG was first activated with PNC to form p-nitrophenyl carbonate conjugates (8PEG-PNC₅) as

previously reported^[41]. Next, the 8PEG-PNC₅ (5.0 g, 1.25 mmol PNC groups) was dissolved in 50 mL of anhydrous dichloromethane, and then, TA (0.33 g, 2.4 mmol) pre-dissolved in 5 mL of anhydrous DMF was added at room temperature. The solution was stirred under a nitrogen atmosphere for 2 h. The product was precipitated in cold diethyl ether, followed by washing with cold ethanol and diethyl ether, and then dried under vacuum for 1 day. The yield was 62% and the degree of substitution with tyramine groups (DS) was 5. The polymer was designated as 8PEGTA₅.

2.3. Hydrogel formation

Solutions containing 6 wt% GelMA or 6 wt% GelMA/2 wt% 8PEGTA₅ were prepared in either PBS or α -MEM (cell experiments) at 37°C. To each solution, LAP as a photoinitiator was added at a concentration of 0.5 wt%. In addition, to the solution containing 6 wt% GelMA/2 wt% 8PEGTA₅, HRP was added at a final concentration of 4 U/mL. To determine the possible phase separation present in the GelMA-8PEGTA mixture, light transmission at 680 nm of solutions prepared at the same concentrations in distilled water was measured using an Agilent UV-Vis spectrometer. In addition, the size distribution of GelMA and GelMA/8PEGTA₅ in aqueous solutions (2 mg/mL) at room temperature was measured by dynamic light scattering (Zetasizer Nano-ZS, Malvern Instruments).

To evaluate the properties of bulk hydrogels, solutions were cast in $1 \times 35 \times 100$ mm (height \times width \times length) PDMS molds and cooled to 22°C to form a physically crosslinked hydrogel. Then, the networks were photo-crosslinked at 365 nm for 1 min in a UV box (intensity of 10 mW/cm², Ultra-Lum, San Diego, USA). A GelMA/8PEGTA₅-IPN hydrogel was formed by submerging the photo-crosslinked network in a 0.03 wt% H_2O_2 solution for 1 min. Finally, all hydrogels were washed with PBS.

2.4. Rheology

To determine the rheological properties of physically crosslinked, photo-crosslinked, and IPN hydrogels, the prepared hydrogels were cut into 25 mm (diameter) disk specimens and tested with a US 200 Rheometer (Anton Paar) using parallel plates (25 mm in diameter) at an initial normal force of 0.2 N. In initial experiments, frequency and strain sweeps were performed at 5°C to determine adequate measuring parameters on hydrogels and were set to a frequency of 0.5 Hz and a strain of 0.5% for all further measurements. Temperature-dependent storage (G') and loss modulus (G'') were measured from 10 to 40°C.

The UV crosslinking kinetics were studied using *in situ* UV curing of 20 mm disks on a 20 mm parallel steel plate

geometry (Discovery HR-1, TA Instruments) at 365 ± 5 nm at room temperature. For all measurements, the gap between the plates was set to 500 μm .

2.5. Compressive and tensile tests

Compression stress-strain analyses were performed on 5×8 mm (height \times diameter) cylindrical specimens in the wet state. Tests were performed at room temperature according to ASTM 695 at a compression rate of 30% per min, $n = 5$. The compressive modulus (E_{c-mod}) was determined at 10% compressive strain.

Tensile stress-strain measurements were performed according to ASTM D 638 using a ZwickRoell tensile tester. Samples with dumbbell shape (50×9 mm) in the wet state were elongated at a speed of 10 mm/min at room temperature. Starting from the initial position (30 mm grip-to-grip separation), the stress and elongation at break of three samples of each gel were measured to obtain values for the tensile modulus (E_{t-mod}) at 10% strain and elongation at break (ϵ_{max}). Tensile and compressive toughness were used as parameters for the resistance to fracture of a hydrogel under stress and determined by integrating the area under the stress-strain curve.

2.6. Gel content and water uptake

The swelling properties of the hydrogels were determined by water uptake and gel content measurements based on gel weights in both swollen and dry states. The gels were first dried for 2 days (m_0), then extracted in water for 2 days (m_s) and eventually dried in an oven at 37°C for 2 days (m_d). All steps were performed at 37°C using three samples of 1×10 mm preformed disks. The water uptake and gel content were calculated according to Equations I and II:

$$\text{Gel content} = \frac{m_d}{m_0} \times 100 \quad (\text{I})$$

$$\text{Water uptake} = \frac{m_s - m_d}{m_d} \times 100 \quad (\text{II})$$

2.7. Microscopic evaluation of the morphology

Cross-sections of the (degraded) hydrogels were imaged by scanning electron microscopy (SEM) using a Jeol JSM-IT100 Scanning Electron Microscope. Degradation was performed by incubation into a 2 U/mL collagenase solution at 37°C (see next section). Hydrogel samples taken at different time points were lyophilized and broken in liquid nitrogen. The cell-printed hydrogels were treated with 10% formaldehyde solution for 2 h at room temperature and dehydrated with 30%, 50%, 70%, 80%,

90%, and 96% ethanol for 30 min each and 100% ethanol twice for 30 min. The constructs were dried with HMDS in a fume hood overnight. The samples were gold sputtered using a Cressington Sputter coater 108 auto before imaging.

2.8. Degradation

Degradation of the photo-crosslinked and IPN hydrogels was tested using 5×8 mm (height \times diameter) cylindrical specimens cast in a PDMS mold. Specimens were dried at 37°C in an oven for 2 days to give the initial weight (m_0). Then, specimens were separately submerged in 2 mL PBS containing 2 U/mL collagenase at 37°C . Sodium azide (0.02 wt%) was added to prevent bacterial growth. The medium was exchanged every 2 days. After 6, 12, 24, 48, 72, 96, 120, and 168 h, specimens ($n = 3$) were removed from the degradation media and washed with deionized water. Thereafter, the specimens were lyophilized to give the dry weight (m_d). The percentage of mass remaining (M_r) was calculated according to Equation III:

$$M_r = \frac{m_d}{m_0} \times 100\% \quad (\text{III})$$

2.9. 3D printing

All printing experiments were performed with an extrusion-based 3D bioprinter (BioMaker 2.0, New Jersey, SunP Biotech Inc., USA) using 6 wt% GelMA or 6 wt% GelMA/2 wt% 8PEGTA₅ solutions to which LAP as a photoinitiator was added at a concentration of 0.5 wt%. In addition, to the 6 wt% GelMA/2 wt% 8PEGTA₅ solution, HRP was added at a final concentration of 4 U/mL. The combination of a printing speed of 4 mm/s and extrusion speed of 0.45 $\mu\text{L/s}$ and needle diameter was optimized. Optimal results were obtained when needles with a diameter of 25G (0.260 ± 0.019 mm, nominal inner diameter) were used. Both larger and smaller diameter needles did not give smooth and regular fibers. The temperature of the nozzle and collecting plate was set at room temperature in line with rheological temperature sweep experiments. The printing speed and extrusion speed were optimized by one-layer ($10 \times 10 \times 0.25$ mm size, line distance of 2 mm) printing tests for both the 6 wt% GelMA and 6 wt% GelMA/2 wt% 8PEGTA₅ solutions (data not shown). The GelMA or GelMA/8PEGTA₅ solution at 37°C was transferred to a syringe (BD, 5 mL, Luer-Lock tip) with dispensing needle. The syringe was kept at 4°C for 10 min to form physical crosslinks followed by 20 min at room temperature for equilibrium. At this temperature, physical crosslinks remain present as shown by the rheological data. On testing, with given GelMA or GelMA/8PEGTA₅ solutions, a printing speed of 4 mm/s and extrusion speed of 0.45 $\mu\text{L/s}$ were chosen for further

experiments. To avoid extrusion of the solution when changing to the next layer, the piston of the syringe was retracted 0.5 mm after printing of each layer. Using these conditions, scaffolds of 10 × 10 mm and a height of 5 mm (20 layers) were printed. UV curing (365 nm) was set at a light intensity of 10 mW/cm² with 5 s irradiation of each two layers during printing. Moreover, UV curing was applied for 1 min after completion of printing. Subsequently, the GelMA/8PEGTA₅ scaffolds were submerged in a 0.03 wt% H₂O₂ solution for 1 min to induce enzymatic crosslinking. The scaffolds were then submerged in PBS and incubated at 37°C overnight. 3D GelMA or GelMA/8PEGTA₅ scaffolds with different geometries were printed for validation.

2.10. Cell culture

Osteosarcoma cells (MG-63 cells), which were selected as the model cell line, were cultured using α -MEM medium supplemented with 10% (v/v) FBS and 1% penicillin and streptomycin in an incubator at 37°C with 5% CO₂. The culture medium was refreshed 3 times a week until the cells reached confluence. On confluence, the cells were trypsinized and counted using a Neubauer cell counting chamber. Cell suspensions with a concentration of 1 × 10⁶ cells/mL in culture medium were used for the preparation of bioinks.

2.11. Bioprinting of bioinks

Macromer stock solutions containing 12 wt% GelMA or 12 wt% GelMA/4 wt% 8PEGTA₅ were prepared using cell culture medium. The solutions were subsequently disinfected using a pasteurization protocol by keeping them at 70°C for 30 min and then at 20°C for 30 min^[42]. This procedure was repeated 3 times. To prepare bioinks containing cells, 2 mL of a macromer stock solution was gently mixed with 2 mL MG-63 suspension (1 × 10⁶ cells/mL) at 37°C and transferred to a 5 mL syringe. The syringe was kept at 4°C for 10 min and mounted in the 3D bioprinter, the chamber temperature was set at 22°C, and the system was incubated for 20 min. The syringe was set to the starting position and printing was carried out using the same procedure as given above for printing without cells. Constructs of 10 × 10 mm and a height of 1 mm (4 layers) were printed in 6-well plates ($n = 4$). After printing, all gels were post-crosslinked with UV (365 ± 5 nm, 10 mW/cm², 1 min). In addition, the GelMA/8PEGTA₅ gels were submerged in PBS containing 0.03 wt% H₂O₂ for 1 min and washed with PBS twice before fresh cell culture medium was added. In the previous research, we have shown that crosslinking of cell-laden tyramine-conjugated natural polymers and 8-arm PEG using HRP at low concentrations of H₂O₂ shows no cytotoxic effects and excellent biocompatibility^[38,43]. The bioprinted constructs

were incubated at 37°C in humidified air (5 vol.%tw CO₂). The medium was refreshed every 2 days. The printing process with cells is graphically illustrated in [Scheme 1](#). The printed scaffolds were placed in culture medium, and the samples were evaluated after 3, 7, and 21 days.

2.12. Live/Dead staining

The live/dead viability/cytotoxicity kit was used to assess cell viability. At scheduled time points, the cells were washed gently with DPBS and 150 μ L of a 2 μ M calcein AM and 4 μ M EthD-1 working solution was added directly to the cells. After incubation for 30 – 45 min at room temperature, the working solution was discarded completely. After rinsing with warm DPBS, the sample was placed on a glass slide to view the labeled cells with fluorescence microscopy (3512001683, Carl Zeiss, Gottingen, Germany).

2.13. Statistics analysis

All data are expressed in mean ± standard deviation. Biochemical assays were performed with triplicate biological sample, if not stated otherwise. Statistical analysis was performed using two-way analysis of variance (ANOVA) with Bonferroni's multiple comparison test ($P < 0.05$), unless otherwise indicated in the figure legends. For all graphs, the following applies: * $P < 0.05$, ** $P < 0.01$, and *** $P < 0.001$.

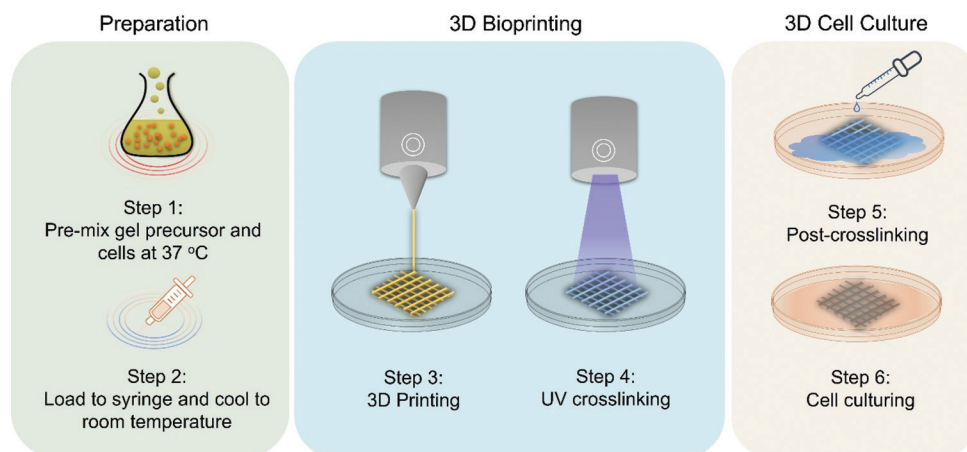
3. Results and discussion

3.1. Synthesis

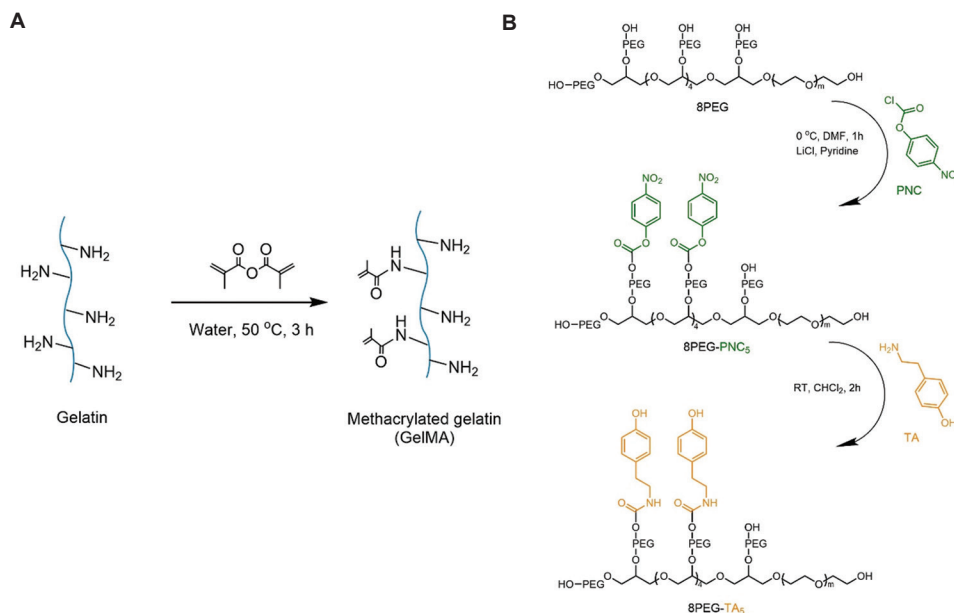
The GelMA was prepared as previously described, and approximately 90% of the lysine amine groups were converted into methacrylamide groups by reacting gelatin with methacrylic anhydride^[20]. The 8PEGTA₅ prepared by activation of the hydroxyl end groups with PNC and subsequent reaction with TA ([Scheme 2](#)) showed the appearance of aromatic protons at 6.79 and 6.99 ppm ([Figure 1](#)). The degree of substitution of the 8PEGTA end groups was determined by comparing the integral values of the aromatic protons with PEG protons, showing that five out of eight hydroxyl end groups were substituted. Using this method, no full conversion of the hydroxyl end groups could be reached even by applying an excess of PNC.

3.2. Crosslinking

Photo-crosslinking of GelMA and the enzymatic crosslinking of phenolic conjugates of synthetic and natural polymers are well-known methods to form hydrogel networks. Both crosslinking mechanisms are radical based. To show the independent crosslinking in macromer mixtures, to form an IPN, by photoinitiation of GelMA and enzymatic crosslinking of the phenolic groups of 8PEGTA₅



Scheme 1. Schematic 3D bioprinting procedure. Step 1: Pre-mix gel precursor and cells at 37°C. Step 2: Load to the syringe at 37°C and cool to room temperature. Step 3: The print head and the base plate are set at 22°C during the printing of a preprogrammed construct. Step 4: Every two layers the hydrogel is irradiated for 5 s by UV light (365 nm). Step 5: For the IPN preparation, the printed hydrogel was submerged in a 0.03 wt% H₂O₂ solution for 1 min after finishing printing. Step 6: Cell culturing of the hydrogel up to 21 days.



Scheme 2. Synthesis of (A) GelMA and (B) 8PEGTA₅.

by HRP in the presence of hydrogen peroxide, two control experiments were performed. A solution of 8PEGTA₅ containing LAP did not form a gel on UV irradiation (experimental details are presented in Supplementary File, Table S1). Second, the potential crosslinking of acrylate groups of GelMA in the presence of HRP was verified. The experiments revealed that no gelation occurred when a solution of H₂O₂ (at a final concentration of 0.03 wt%) was added to a 6 wt% solution of GelMA containing 4 U/mL HRP, which is in accordance with results of Danielson *et al.* who showed that a mediator like acetyl acetone is necessary to induce crosslinking of acrylates^[44].

Consecutively, physically crosslinked hydrogels, photo-crosslinked hydrogels, and IPNs, as schematically depicted in Scheme 3, were formed.

3.3. Solution properties and printability

The favorable use of GelMA-based solutions for 3D bioprinting applications is due to the exploitation of its temperature-dependent physical gelation properties. GelMA is well soluble in aqueous solutions at higher temperatures, allowing these pre-gelation solutions to form stable 3D structures on cooling. An important parameter in the printability of GelMA-based bioinks

is the macromer concentration. Recent investigations have shown that printing of GelMA can be performed at concentrations ranging from 5 wt% to 15 wt%, providing constructs with promising stability and cell viability^[34,35]. Moreover, it was shown that cell viability drastically decreased with increasing GelMA concentration, while too low GelMA concentrations led to poor printing ability^[36,37]. In a previous study by Wang *et al.*^[43], it was shown that tyramine conjugated of 8PEGTA₅ can be enzymatically crosslinked using HRP as a catalyst in the presence of H₂O₂. The gel obtained at a concentration of 10 wt% is highly elastic. Although such a gel is cytocompatible

and shows promising results as a matrix for cartilage tissue regeneration, it shows a lower metabolic activity of encapsulated human mesenchymal stem cells. In addition, it was also shown that co-crosslinking of the 8PEGTA₅ with a hyaluronic acid tyramine conjugate improves the biological performance of the hydrogel. The lowest concentration of the 8PEGTA₅ that can form a gel at low enzyme and H₂O₂ concentration was 2 wt%.

In preliminary experiments, it was shown that in the temperature window just below the gel point of a 6 wt% GelMA solution at 27°C, smooth and continuous filaments could be extruded through a fine needle (25G). At lower temperatures, the increasing gel strength led to non-continuous, curled, and irregular filaments. At 30°C, which is higher than the gel point, the inks were liquid-like, and no continuous filaments were formed (Figure S1, Supplementary File).

Similar experiments were performed on mixtures of GelMA and the 8PEGTA₅. As reported in the previous studies, depending on concentration, aqueous solutions of gelatin or GelMA and PEG or PEG derivatives are turbid indicating that phase separation has taken place^[12,38,39]. This phase separation can lead to poor physical gelation of the GelMA and consequently to non-printability of solutions or bioinks. It was observed that solutions containing 6 wt% GelMA and 2 wt% 8PEGTA₅ were transparent but became translucent at higher 8PEGTA₅ concentrations. The light transmission of a 6 wt% GelMA/2 wt% 8PEGTA₅ solution in water at 680 nm was 85%, slightly lower than that of a 6 wt% GelMA solution (89%). Moreover, intensity plots from dynamic light scattering (DLS) measurements at high dilution revealed the presence of particles mainly with an average size of 70 nm (Figure S2, Supplementary File). These data indicated the occurrence of only microphase separation in an aqueous solution of 6 wt% GelMA/2 wt% 8PEGTA₅. The gel point of this

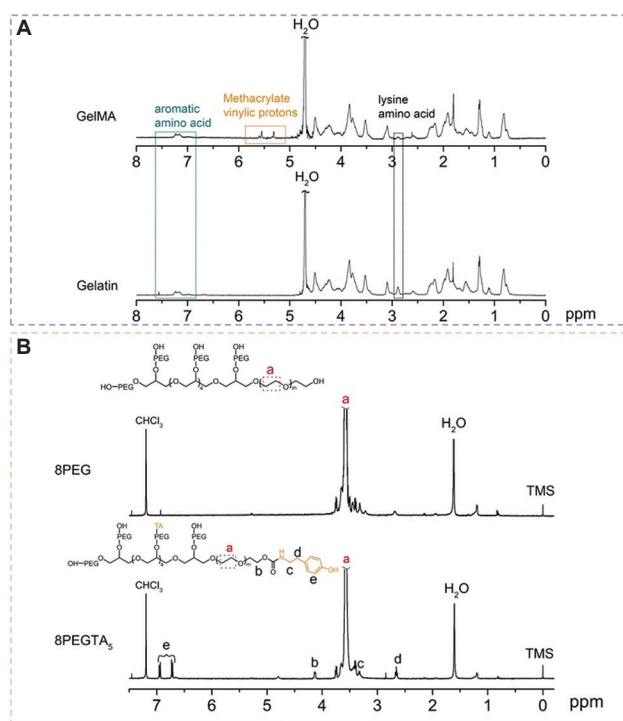


Figure 1. ¹H-NMR spectra of GelMA (A, top) and gelatin (A, bottom) in D₂O and 8PEG (B, top) and 8PEGTA₅ (B, bottom) in CDCl₃.

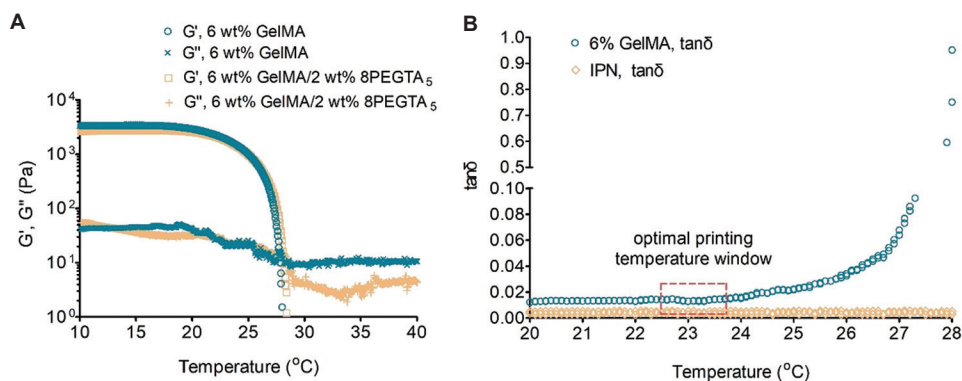


Figure 2. (A) Storage (G') and loss modulus (G'') of 6 wt% GelMA and 6 wt% GelMA/2 wt% 8PEGTA₅ physically crosslinked hydrogels as a function of temperature. (B) Optimal printing temperature window based on $\tan \delta$ value of 6 wt% GelMA and IPN.

macromer mixture is almost the same as of the 6 wt% GelMA solution and similarly as described above, smooth

and continuous filaments could be extruded through a fine needle (25G) in the temperature window just below the gel point (Figure S1, Supplementary File). Based on these results, we compared the properties of 6 wt% GelMA and 6 wt% GelMA/2 wt% 8PEGTA₅ gels.

3.4. Gel content and swelling

To determine the swelling of the photo-crosslinked 6 wt% GelMA (GelMA-UV) and 6 wt% GelMA/2 wt% 8PEGTA₅ IPN (GelMA/8PEGTA₅-IPN) hydrogels, macromer solutions were placed in a cylindrical mold at 37°C and cooled to room temperature to give physically crosslinked networks. Subsequent light exposure (365 nm) induced photo-crosslinking of the GelMA. In case of the GelMA/8PEGTA₅ macromer mixture, which also contains HRP (4 U/mL), after UV crosslinking, a second enzymatically crosslinked network was formed by incubating the hydrogel in a 0.03 wt% H₂O₂ solution. The gel content and water uptake of the GelMA-UV and GelMA/8PEGTA₅-IPN hydrogels are given in Table 1. All hydrogels had a gel content higher than 86%. The higher macromer concentration by addition of 8PEGTA₅ to the GelMA provided a higher crosslinking density, leading to

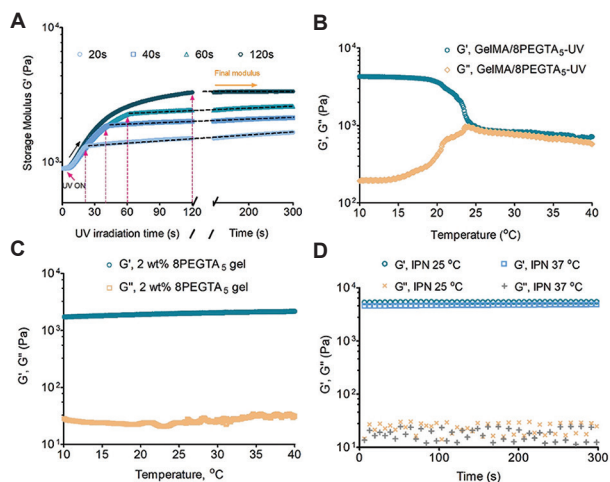
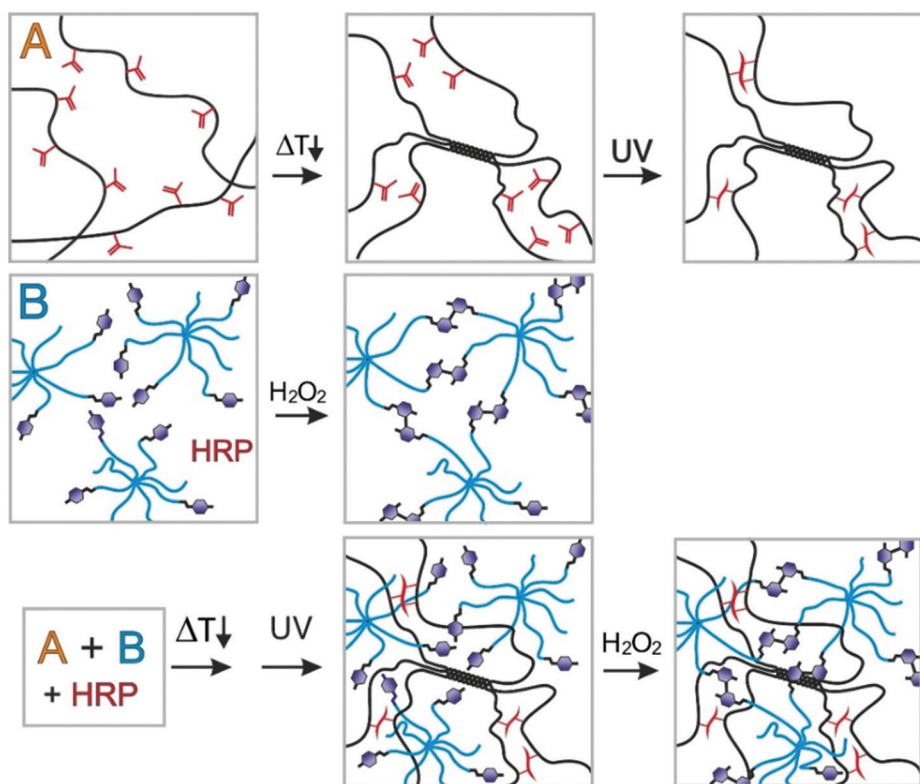


Figure 3. (A) UV crosslinking kinetics: Storage modulus as a function of UV irradiation (375 nm) time of GelMA/8PEGTA₅ at 22°C. (B) Temperature sweep of the chemically crosslinked GelMA/8PEGTA₅ (2 min UV irradiation). (C) Temperature sweep of a 2 wt% 8PEGTA₅ gel formed by enzymatic crosslinking. (D) Storage modulus (G') and loss modulus (G'') of the GelMA/8PEGTA₅-IPN at 25 and 37°C.



Scheme 3. Top row: Physical and subsequent UV crosslinking of GelMA; middle row: Enzymatic crosslinking of 8PEGTA₅ by HRP in the presence of hydrogen peroxide; bottom row: IPN formation, by consecutive physical and UV crosslinking of the GelMA and enzymatic post-crosslinking, of a mixture of GelMA, 8PEGTA₅, and HRP.

Table 1. Water uptake and gel content of GelMA and GelMA/8PEGTA₅-IPN hydrogels.

Network	Photograph ^a	Gel content (%)	Water uptake (%)
GelMA-UV		86±3	1730±180***
GelMA/8PEGTA ₅ -IPN		91±3*	665±6

^aScale is in mm. * $P < 0.05$, *** $P < 0.001$, $n = 5$

a decreased water uptake. Interestingly, the GelMA-UV gel was transparent after gelation and photo-crosslinking whereas the GelMA/8PEGTA₅-IPN was turbid. The IPNs showed a significantly lower swelling (665%) compared to GelMA-UV networks (1730%).

3.5. Rheology

At the optimized concentration and temperature for deposition of stable printed fibers, mechanical properties of the physically crosslinked, photo-crosslinked, and IPN hydrogels were determined by rheology. First, strain and frequency sweeps of physically crosslinked GelMA and GelMA/8PEGTA₅ were recorded at 5°C. Strains of maximally 0.5% could be applied before deformation occurred and a gel-sol transition at higher strains was observed for both gels. At a constant strain of 0.5%, the physically crosslinked gels showed minor dependence of G' and G'' on the frequency (Figure S3, Supplementary File). The storage (G') and loss modulus (G'') of these physically crosslinked hydrogels as a function of temperature are presented in Figure 2A. The complex viscosity of GelMA and GelMA/8PEGTA₅ solutions showed no difference as a function of temperature (Figure S4, Supplementary File). The gel point, $G' = G''$, for both systems is observed at 27°C. The appropriate printing temperature can be visualized by the loss tangent ($\tan\delta$) of the inks, the ratio of loss modulus (G'') and storage modulus (G'), representing the plasticity and elasticity of materials^[40]. As shown in Figure 2B, at higher temperatures ($G' < G''$), the ink will show a typical liquid-like behavior, and no filaments can be formed during printing. On cooling, G' increases and at temperatures below the gel point, a temperature window for optimal printing is present.

By the foregoing experiments, it was shown that the rheological properties and printing behavior of the GelMA

and GelMA/8PEGTA₅ physically crosslinked hydrogels were optimal at a temperature of 22°C. Subsequently, the rheological properties of the hydrogels formed after UV crosslinking (GelMA-UV) and UV and enzymatic crosslinking (GelMA/8PEGTA₅-IPN) were determined. In these experiments, the GelMA/8PEGTA₅ solution contains both LAP as a photoinitiator and a low concentration of the enzyme HRP. Incubating the photo-crosslinked hydrogel in a hydrogen peroxide solution, the second crosslinking step afforded the IPN (Scheme 3).

The kinetics of UV irradiation in the physically crosslinked GelMA/8PEGTA₅ hydrogel at room temperature was determined by measuring the changes in the rheological properties upon *in situ* UV irradiation. With increasing the irradiation time from 20 s to 120 s, the storage modulus of IPN gels increased from 1.67 KPa to 3.35 KPa (Figure 3A). Interestingly, after shutting down each UV irradiation, the storage modulus was still increasing as function of time sweep. This indicates with insufficient UV irradiation, the double bonds presence in precursor could not fully reacted. As depicted in Figure 3A, dash line, an optimal time for UV crosslinking using LAP as a photoinitiator appeared to be 2 min, as indicated by plateau that was observed after irradiation. Longer times did not significantly increase the storage modulus of the gel. A temperature sweep from 10 to 40°C of the GelMA/8PEGTA₅ hydrogel after UV crosslinking revealed a drop in the storage modulus in the range of 25 – 30°C due to loss of the gelatin physical crosslinks (Figure 3B). At a temperature of 37°C, the photo-crosslinked GelMA/8PEGTA₅ hydrogel showed G' and G'' values close to each other indicating a soft viscous gel. Such printed scaffolds were expected to have low shape stability upon implantation^[37]. In a control experiment, within the temperature range of 10 – 40°C, an enzymatically crosslinked 2 wt% 8PEGTA₅ hydrogel showed no changes in the storage and loss modulus (Figure 3C). The GelMA/8PEGTA₅ gel was subsequently submerged in 0.03 wt% H₂O₂ solution in PBS to enzymatically crosslink the 8PEGTA₅ conjugate to form the IPN. The enzymatic crosslinking is very fast and within seconds the storage modulus reached a maximum value of 6 kPa. IPN gels showed mechanical properties independent of temperatures up to 37°C (Figure 3D).

3.6. Compression and tensile properties

Representative compressive and tensile stress-strain curves for all gels are depicted in Figure 4. A reduced swelling behavior and increased mechanical properties of hydrogels are expected with increasing concentration and degree of crosslinking.

Compressive and tensile tests of the IPN showed significantly higher compressive and tensile toughness than that of the pure GelMA-UV hydrogel (Table 2). Based on the literature, the compressive modulus of hydrogels prepared from 5 to 10 wt% GelMA with high functionalization (>75%) range from 5 kPa to 20 kPa and the tensile modulus range from 15 to 35 kPa^[13,45,46]. The photo-crosslinked GelMA-UV hydrogel was easy to deform compared to the IPN and had a low compressive ($E_{C-mod} = 21 \pm 6$ kPa) and tensile ($E_{T-mod} = 33 \pm 6$ kPa) modulus, similar to reported values, whereas the IPN E_C and E_T were 82 ± 2 and 111 ± 4 kPa, respectively. The tensile and compressive tests showed that the IPN withstands both high stresses and high strains compared to the GelMA-UV hydrogels. In the IPN, the GelMA and 8PEGTA₅ networks integrate both rigid and elastic properties^[35,47]. The compressive and tensile toughness of the IPN were 5.98 ± 0.56 and 2.93 ± 0.60 N/mm², whereas the compressive and tensile toughness of the GelMA-UV hydrogels were 1.66 ± 0.21 and 0.48 ± 0.11 N/mm².

3.7. Degradation

The mass remaining and morphology of the hydrogels on degradation in the presence of collagenase (2 U/mL

collagenase at 37°C) were monitored in time (Figure 5A). Within 25 h, the GelMA hydrogel was almost fully degraded. Compared to the initial specimen, the shape of this hydrogel already deformed at 6 h. The SEM image in Figure 5B showed that after 6 h degradation, the patchy pores in the gel had been progressively degraded, with appearance from the initially small porous structure to the macroporous structure. The integrity of the IPN hydrogel remained, and the samples became more transparent in time (Figure 5B, insets). The initially whitish samples, likely due to micro phase separation, became fully transparent after 168 h incubation time, which according to degradation profile of GelMA has completely degraded. We infer that the remaining porous structure is from the 8PEGTA₅ enzymatic crosslinking. The approximately 30% remaining weight is close to the mass ratio of 8PEGTA₅ (25%). The change into a fully transparent gel indicated that the 8PEGTA₅ was present as a second network and only the GelMA network was fully degraded. The remaining 8PEGTA₅ gel is slowly degraded and no gel was observed after 8 weeks (Figure S5, Supplementary File).

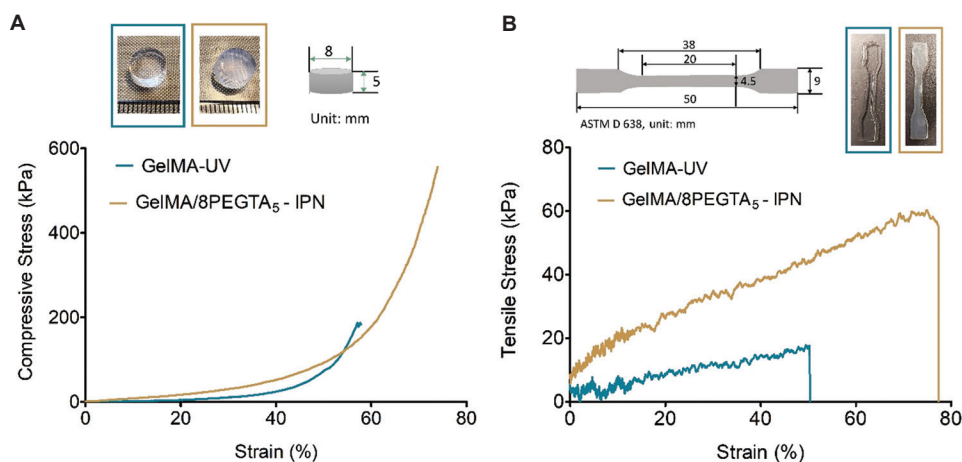


Figure 4. Stress-strain curves (wet state) of GelMA-UV and GelMA/8PEGTA₅-IPN hydrogels in compression (A) and elongation (B). The tests were performed at room temperature ($n = 5$).

Table 2. Compressive and tensile properties of a photo-crosslinked single network (GelMA-UV) and double crosslinked network (IPN).

Network	Compressive modulus (E_{C-mod}) (kPa)	Average fracture force (N)	Average fracture strain (%)	Compressive toughness (N/mm ²)
GelMA-UV	21±6	10.52±0.12	52.12±0.33	1.66±0.21
GelMA/8PEG-TA ₅ -IPN	82±2***	28.63±0.80	64.73±0.52	5.98±0.56**
Network	Tensile modulus (E_{T-mod}) (kPa)	Average fracture force (N)	Average fracture strain (%)	Tensile toughness (N/mm ²)
GelMA-UV	33±6	0.07±0.01	48.43±4.05	0.48±0.11
GelMA/8PEG-TA ₅ -IPN	111±4***	0.24±0.01	71.25±5.14	2.93±0.60**

** $P < 0.01$, *** $P < 0.001$, $n = 5$

3.8. Printability of GelMA and GelMA/PEGTA₅ solutions and bioinks

The GelMA and GelMA/8PEGTA₅ hydrogel precursor solutions, using PBS as a solvent, could be successfully printed with high shape fidelity (Figure S6, Supplementary File). On printing GelMA, the physically crosslinked network formed at room temperature supported at least two layers, and intermediate 5 s UV crosslinking created a stable

structure. The scaffold was post-UV crosslinked for 2 min. Applying similar printing parameters with intermediate UV crosslinking and post-UV curing, stable structures could be prepared from GelMA/8PEGTA₅. The scaffold was then submerged in a 0.03 wt% H₂O₂ solution to create the IPN filaments.

GelMA-UV and GelMA/8PEGTA₅-IPN scaffolds of cubic shape are shown in Figure 6A. According to preset

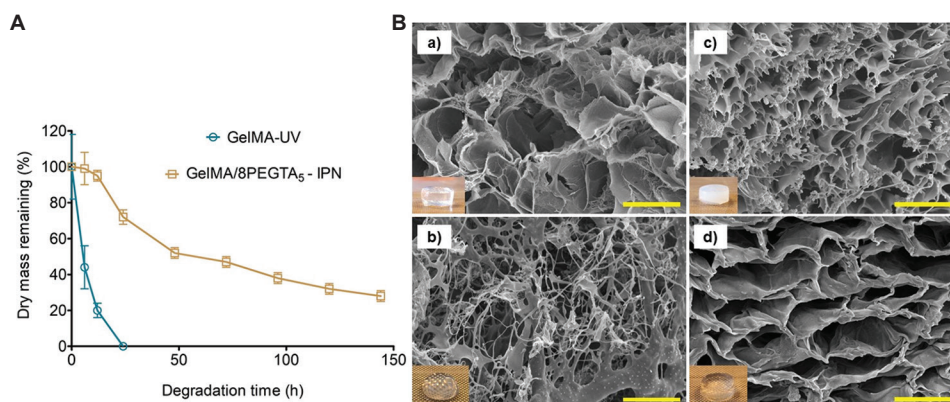


Figure 5. (A) Mass remaining of the photo-crosslinked GelMA gel and GelMA/8PEGTA₅-IPN gel as a function of degradation time. (B) Morphology of (a) GelMA at 0 h and (c) IPN hydrogels at 0 h, (b) GelMA after 6 h, and (d) IPN after 168 h of degradation. Scale bar: 100 μ m. Scale bar of the inset: 1 mm.

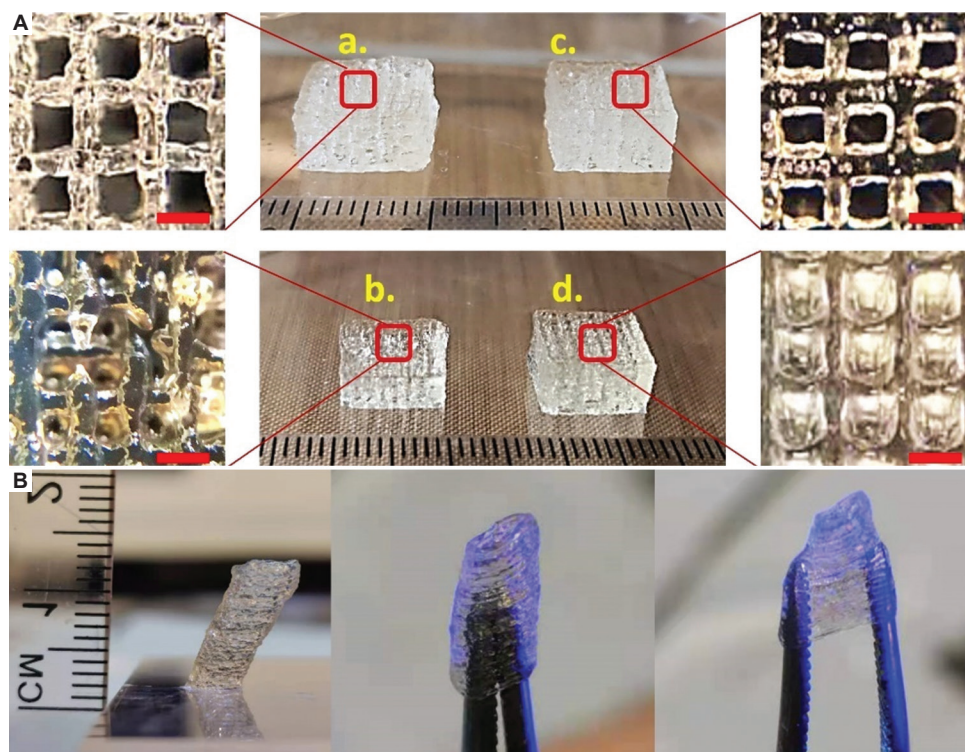


Figure 6. (A) Images of 3D scaffolds printed from (a) GelMA and (b) GelMA after incubating at 37°C in PBS overnight, and (c) GelMA/8PEGTA₅ and (d) GelMA/8PEGTA₅ after incubating at 37°C in PBS overnight (scale bar: 1 mm). (B) 3D-printed inclined tubular scaffold from GelMA/8PEGTA₅-IPN and similar tubular scaffold before and after stretching using tweezers. Videos of printing constructs with an inclined tubular structure in air and gel bath are uploaded with descriptions presented in the Supplementary File (Video clip S1).

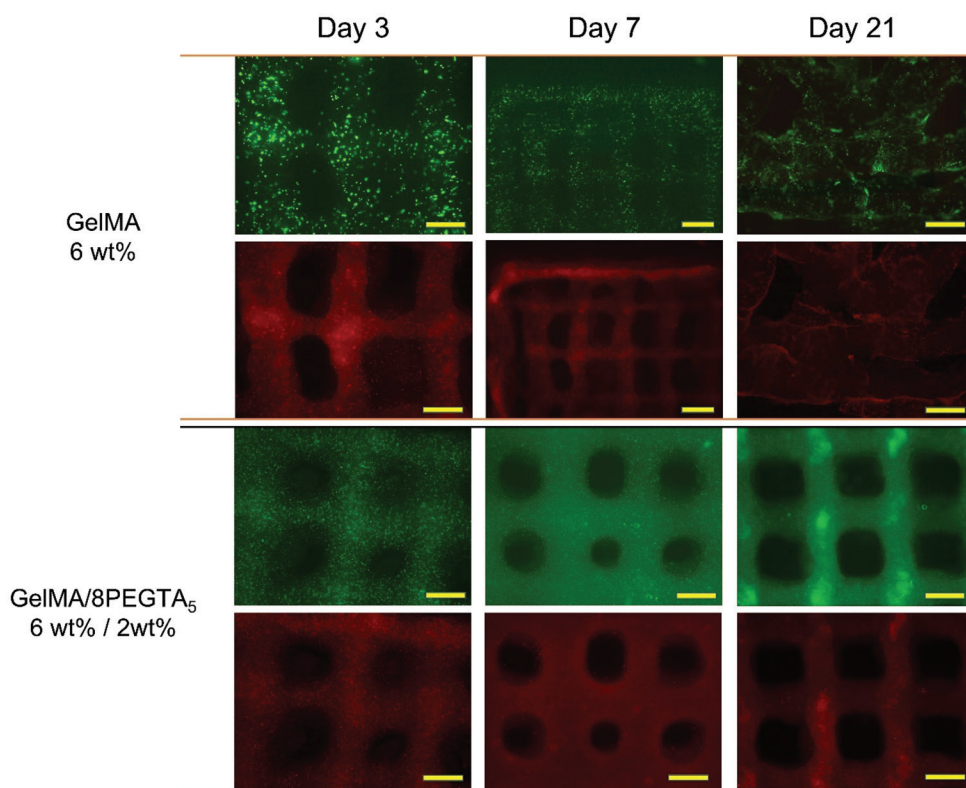


Figure 7. Live/dead images of cultured MG-63 cells in hydrogels for 3, 7, and 21 days (scale bar: 500 μm).

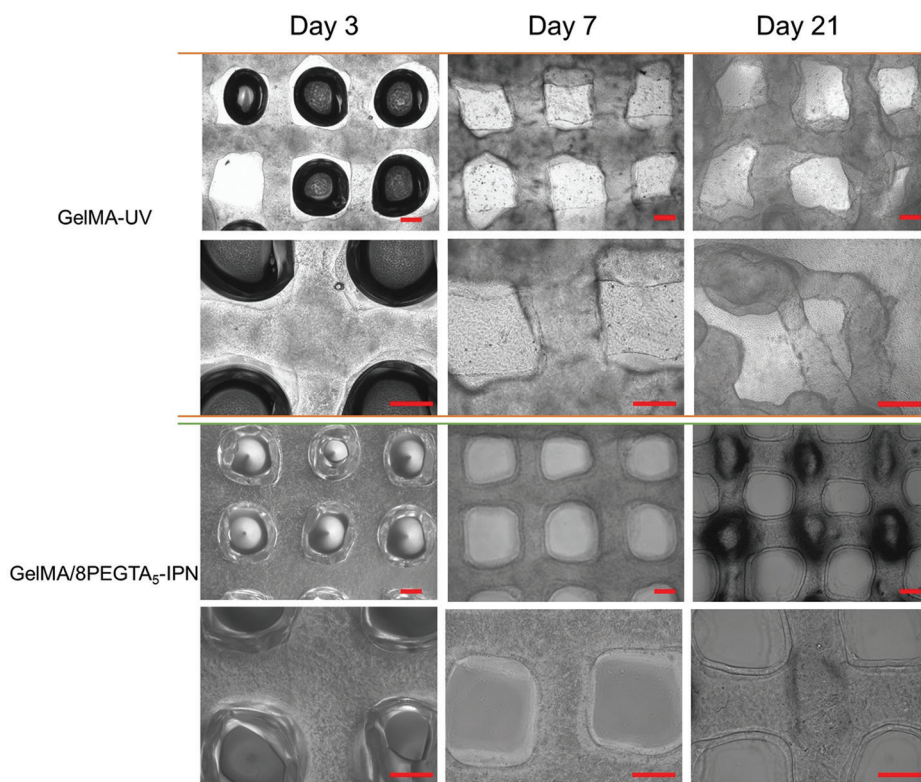


Figure 8. Brightfield images of cultured MG-63 cells in the hydrogels for 3, 7, and 21 days (scale bar: 500 μm).

parameters, filaments were deposited at 1.5 mm line distance, and regular structures with cubic pores were built. On incubation of the scaffolds in water at 37°C overnight, the photo-crosslinked GelMA-UV scaffold was destructed compared to the scaffold just after printing (Figure 6Aa and 6Ab). It could be seen that in the center part, some of the filaments were broken. Under similar conditions, the printed IPN-type scaffold retained its shape and pore structure, showing good structural stability (Figure 6Ac and 6Ad). The demonstrated inclined tubular structure was printed with GelMA/8PEGTA₅. The IPN-type scaffold showed high elasticity on deformation (Figure 6B).

To investigate the potentially harmful effects of the solution components and extrusion parameters on cell viability, preliminary bioprinting experiments using osteosarcoma cells (MG-63)-laden gel precursors were consecutively carried out. Cubic structures (10 mm × 10 mm, thickness 2 mm) were printed as a typical 3D model. Both in GelMA and GelMA/8PEGTA₅ bioprinted structures, MG-63 cells were homogeneously distributed, indicating homogeneous mixing of the cells in the bioinks (Figure 7). A live-dead assay, in which green indicates live cells and red dead cells, revealed that on day 3, more dead cells were observed than on days 7 and 21, which may be attributed to extrusion stress during printing and the long operational time due to physical gelation of the GelMA. However, after culturing for 7 and 21 days, around 90% of the cells were alive. It was also noted that after culturing for 3 days, cells in the printed GelMA construct had a round shape and part of the cells started to spread. After 21 days of culturing, cells in the GelMA construct had fully spread and started to connect with each other. In the IPN hydrogel, this process was slower. After 3 and 7 days, cells in the IPN maintained a round shape and even at 21 days of culturing, cells hardly started to spread (Figure S7, Supplementary File). These results further indicate that the IPN bioinks have excellent integrity for bioprinting of constructs that aim for longer cell culture applications. The brightfield images (Figure 8) of printed constructs were monitored during cell culturing, which clearly demonstrated the shape fidelity during cell proliferation and constructs degradation.

4. Conclusion

In this paper, we report the development of inks composed of GelMA and 8-arm PEGTA conjugates. An IPN of GelMA/8PEGTA₅ was created by subsequent photo-crosslinking and enzymatic crosslinking. Compared to the GelMA network, the IPN showed increased stability and slower degradation, and appeared an easy-to-print ink for bioprinting applications. The results from cell viability analyses of MG-63 cell-laden 3D-printed hydrogels were promising. However, to prepare custom bioinks, testing

remains necessary to optimize printing parameters when using different cell types. Different applications may require different scaffold mechanical properties and degradation times. Varying the composition and degree of substitution of GelMA and multi-arm PEGTA, as well as using other tyramine-conjugated water-soluble compounds, may result in the creation of IPNs with a wide range of properties. The GelMA/8PEGTA₅ ink has a high potential to generate cell-laden bioinks for extrusion-based bioprinting. Such 3D constructs can be applied for regeneration of tissues like blood vessels and can also be used for fundamental studies on tumor models and drug delivery applications.

Acknowledgments

We would like to acknowledge SunP Biotechnology for providing BioMaker as printing tool and SunP Float as gel bath for this work.

Funding

We would like to acknowledge the Chinese Scholarship Council for financial support (personal grant to J. Liang, no. 201608440247).

Conflict of interest

The authors declare that they have no known competing financial interests or personal relationships that could have appeared to influence the work reported in this paper.

Author contributions

Conceptualization: Rong Wang, Jia Liang, and Piet J. Dijkstra

Investigation: Rong Wang, Jia Liang, and Zhule Wang

Writing – original draft: All authors

Writing – review and editing: Rong Wang, Piet J. Dijkstra

All authors have given approval to the final version of the manuscript.

Ethics approval and consent to participate

Not applicable.

Consent for publication

Not applicable.

Availability of data

The data presented in this study are available on request from the corresponding author.

References

1. Hoffman AS, 2002, Hydrogels for biomedical applications. *Adv Drug Deliv Rev*, 54: 3–12.

- [https://doi.org/10.1016/s0169-409x\(01\)00239-3](https://doi.org/10.1016/s0169-409x(01)00239-3)
- Guan XF, Avci-Adali M, Alarcin E, *et al.*, 2017, Development of hydrogels for regenerative engineering. *Biotechnol J*, 12:1600394.
<https://doi.org/10.1002/biot.201600394>
 - Ouyang L, Highley CB, Sun W, *et al.*, 2017, A generalizable strategy for the 3D bioprinting of hydrogels from nonviscous photo-crosslinkable inks. *Adv Mater*, 29: 1604983.
<https://doi.org/10.1002/adma.201604983>
 - Annabi N, Tamayol A, Uquillas JA, *et al.*, 2014, 25th anniversary article: Rational design and applications of hydrogels in regenerative medicine. *Adv Mater*, 26: 85–123.
<https://doi.org/10.1002/adma.201303233>
 - Hoch E, Hirth T, Tovar GE, *et al.*, 2013, Chemical tailoring of gelatin to adjust its chemical and physical properties for functional bioprinting. *J Mater Chem B*, 1: 5675–5685.
<https://doi.org/10.1039/C3TB20745E>
 - Billiet T, Gevaert E, De Schryver T, *et al.*, 2014, The 3D printing of gelatin methacrylamide cell-laden tissue-engineered constructs with high cell viability. *Biomaterials*, 35: 49–62.
<https://doi.org/10.1016/j.biomaterials.2013.09.078>
 - O'Connell CD, Onofrillo C, Duchi S, *et al.*, 2019, Evaluation of sterilisation methods for bio-ink components: Gelatin, gelatin methacryloyl, hyaluronic acid and hyaluronic acid methacryloyl. *Biofabrication*, 11: 035003.
<https://doi.org/10.1088/1758-5090/ab0b7c>
 - Choi JR, Yong KW, Choi JY, *et al.*, 2019, Recent advances in photo-crosslinkable hydrogels for biomedical applications. *Biotechniques* 66: 40–53.
<https://doi.org/10.2144/btn-2018-0083>
 - Schuurman W, Levett PA, Pot MW, *et al.*, 2013, Gelatin-methacrylamide hydrogels as potential biomaterials for fabrication of tissue-engineered cartilage constructs. *Macromol Biosci*, 13: 551–561.
<https://doi.org/10.1002/mabi.201200471>
 - Klotz BJ, Gawlitta D, Rosenberg AJ, *et al.*, 2016, Gelatin-methacryloyl hydrogels: Towards biofabrication-based tissue repair. *Trends Biotechnol*, 34: 394–407.
<https://doi.org/10.1016/j.tibtech.2016.01.002>
 - Yue K, Trujillo-de Santiago G, Alvarez MM, *et al.*, 2015, Synthesis, properties, and biomedical applications of gelatin methacryloyl (GelMA) hydrogels. *Biomaterials*, 73: 254–271.
<https://doi.org/10.1016/j.biomaterials.2015.08.045>
 - Liang J, Guo Z, Timmerman A, *et al.*, 2019, Enhanced mechanical and cell adhesive properties of photo-crosslinked PEG hydrogels by incorporation of gelatin in the networks. *Biomed Mater*, 14: 024102.
<https://doi.org/10.1088/1748-605X/aaf31b>
 - Yoon HJ, Shin SR, Cha JM, *et al.*, 2016, Cold water fish gelatin methacryloyl hydrogel for tissue engineering application. *PLoS One*, 11: e0163902.
<https://doi.org/10.1371/journal.pone.0163902>
 - Zhu M, Wang Y, Ferracci G, *et al.*, 2019, Gelatin methacryloyl and its hydrogels with an exceptional degree of controllability and batch-to-batch consistency. *Sci Rep*, 9: 6863.
<https://doi.org/10.1038/s41598-019-42186-x>
 - Bakaic E, Smeets NM, Hoare T, 2015, Injectable hydrogels based on poly(ethylene glycol) and derivatives as functional biomaterials. *RSC Adv*, 5: 35469–35486.
<https://doi.org/10.1039/C4RA13581D>
 - Moore EM, West JL, 2019, Bioactive poly(ethylene glycol) acrylate hydrogels for regenerative engineering. *Regen Eng Transl Med*, 5: 167–179.
<https://doi.org/10.1007/s40883-018-0074-y>
 - Ooi HW, Kocken JM, Morgan FL, *et al.*, 2020, Multivalency enables dynamic supramolecular host-guest hydrogel formation. *Biomacromolecules*, 21: 2208–2217.
<https://doi.org/10.1021/acs.biomac.0c00148>
 - Sim SL, He T, Tscheliessnig A, *et al.*, 2012, Branched polyethylene glycol for protein precipitation. *Biotechnol Bioeng*, 109: 736–746.
<https://doi.org/10.1002/bit.24343>
 - Wang J, Zhang F, Tsang WP, *et al.*, 2017, Fabrication of injectable high strength hydrogel based on 4-arm star PEG for cartilage tissue engineering. *Biomaterials*, 120: 11–21.
<https://doi.org/10.1016/j.biomaterials.2016.12.015>
 - Skardal A, Devarasetty M, Kang HW, *et al.*, 2015, A hydrogel bioink toolkit for mimicking native tissue biochemical and mechanical properties in bioprinted tissue constructs. *Acta Biomater*, 25: 24–34.
<https://doi.org/10.1016/j.actbio.2015.07.030>
 - Rutz AL, Hyland KE, Jakus AE, *et al.*, 2015, A multilateral bioink method for 3D printing tunable, cell-compatible hydrogels. *Adv Mater*, 27: 1607–1614.
<https://doi.org/10.1002/adma.201405076>
 - Liang J, Dijkstra PJ, Poot AA, *et al.*, 2022, Hybrid hydrogels based on methacrylate-functionalized gelatin (GelMA) and synthetic polymers. *Biomed Mater Devices*.
<https://doi.org/10.1007/s44174-022-00023-2>
 - Pereira RF, Bartolo PJ, 2015, 3D bioprinting of photocrosslinkable hydrogel constructs. *J Appl Polym Sci*, 132: 42458–42473.
<https://doi.org/10.1002/app.42458>

24. Decante G, Costa JB, Silva-Correia J, *et al.*, 2021, Engineering bioinks for 3D bioprinting. *Biofabrication*, 13: 032001.
<https://doi.org/10.1088/1758-5090/abec2c>
25. Gao G, Yonezawa T, Hubbell K, *et al.*, 2015, Inkjet-bioprinted acrylated peptides and PEG hydrogel with human mesenchymal stem cells promote robust bone and cartilage formation with minimal printhead clogging. *Biotechnol J*, 10: 1568–1577.
<https://doi.org/10.1002/biot.201400635>
26. Daniele MA, Adams AA, Naciri J, *et al.*, 2014, Interpenetrating networks based on gelatin methacrylamide and PEG formed using concurrent thiol click chemistries for hydrogel tissue engineering scaffolds. *Biomaterials*, 35: 1845–1856.
<https://doi.org/10.1016/j.biomaterials.2013.11.009>
27. Pacelli S, Rampetsreiter K, Modaresi S, *et al.*, 2018, Fabrication of a double-cross-linked interpenetrating polymeric network (IPN) hydrogel surface modified with polydopamine to modulate the osteogenic differentiation of adipose-derived stem cells. *ACS Appl Mater Interfaces*, 10: 24955–24962.
<https://doi.org/10.1021/acsami.8b05200>
28. Schipani R, Scheurer S, Florentin R, *et al.*, 2020, Reinforcing interpenetrating network hydrogels with 3D printed polymer networks to engineer cartilage mimetic composites. *Biofabrication*, 12: 035011.
<https://doi.org/10.1088/1758-5090/ab8708>
29. Zhang X, Kim GJ, Kang MG, *et al.*, 2018, Marine biomaterial-based bioinks for generating 3D printed tissue constructs. *Mar Drugs*, 16: 484.
<https://doi.org/10.3390/md16120484>
30. Jeon O, Shin JY, Marks R, *et al.*, 2017, Highly elastic and tough interpenetrating polymer network-structured hybrid hydrogels for cyclic mechanical loading-enhanced tissue engineering. *Chem Mater*, 29: 8425–8432.
<https://doi.org/10.1021/acs.chemmater.7b02995>
31. Seyedmahmoud R, Çelebi-Saltik B, Barros N, *et al.*, 2019, Three-dimensional bioprinting of functional skeletal muscle tissue using gelatin methacryloyl-alginate bioinks. *Micromachines (Basel)*, 10: 679.
<https://doi.org/10.3390/mi10100679>
32. Fares MM, Sani ES, Lara RP, *et al.*, 2018, Interpenetrating network gelatin methacryloyl (GelMA) and pectin-g-PCL hydrogels with tunable properties for tissue engineering. *Biomater Sci*, 6: 2938–2950.
<https://doi.org/10.1039/c8bm00474a>
33. Berger AJ, Linsmeier KM, Kreeger PK, *et al.*, 2017, Decoupling the effects of stiffness and fiber density on cellular behaviors via an interpenetrating network of gelatin-methacrylate and collagen. *Biomaterials*, 141: 125–135.
<https://doi.org/10.1016/j.biomaterials.2017.06.039>
34. Xiao W, He J, Nichol JW, *et al.*, 2011, Synthesis and characterization of photocrosslinkable gelatin and silk fibroin interpenetrating polymer network hydrogels. *Acta Biomater*, 7: 2384–2393.
<https://doi.org/10.1016/j.actbio.2011.01.016>
35. Shin H, Olsen BD, Khademhosseini A, 2012, The mechanical properties and cytotoxicity of cell-laden double-network hydrogels based on photocrosslinkable gelatin and gellan gum biomacromolecules. *Biomaterials*, 33: 3143–3152.
<https://doi.org/10.1016/j.biomaterials.2011.12.050>
36. Serban MA, Kaplan DL, 2010, pH-sensitive ionomeric particles obtained via chemical conjugation of silk with poly(amino acid)s. *Biomacromolecules*, 11: 3406–3412.
<https://doi.org/10.1021/bm100925s>
37. Park KM, Ko KS, Joung YK, *et al.*, 2011, *In situ* cross-linkable gelatin-poly(ethylene glycol)-tyramine hydrogel via enzyme-mediated reaction for tissue regenerative medicine. *J Mater Chem*, 21: 13180–13187.
<https://doi.org/10.1039/C1JM12527C>
38. Jin R, Teixeira LS, Dijkstra PJ, *et al.*, 2010, Enzymatically-crosslinked injectable hydrogels based on biomimetic dextran-hyaluronic acid conjugates for cartilage tissue engineering. *Biomaterials*, 31: 3103–3113.
<https://doi.org/10.1016/j.biomaterials.2010.01.013>
39. Wang R, Leber N, Buhl C, *et al.*, 2014, Cartilage adhesive and mechanical properties of enzymatically crosslinked polysaccharide tyramine conjugate hydrogels. *Polym Advan Technol*, 25: 568–574.
<https://doi.org/10.1002/pat.3286>
40. Wei Q, Xu M, Liao C, *et al.*, 2016, Printable hybrid hydrogel by dual enzymatic polymerization with superactivity. *Chem Sci*, 7: 2748–2752.
<https://doi.org/10.1039/C5SC02234G>
41. Wang R, Both SK, Geven M, *et al.*, 2015, Kinetically stable metal ligand charge transfer complexes as crosslinks in nanogels/hydrogels: Physical properties and cytotoxicity. *Acta Biomater*, 26: 136–144.
<https://doi.org/10.1016/j.actbio.2015.08.019>
42. Fantini V, Bordoni M, Scocozza F, *et al.*, 2019, Bioink composition and printing parameters for 3D modeling neural tissue. *Cells*, 8:830.
<https://doi.org/10.3390/cells8080830>
43. Wang R, Huang X, Zoetebier B, *et al.*, 2023, Enzymatic co-crosslinking of star-shaped poly(ethylene glycol) tyramine and hyaluronic acid tyramine conjugates provides elastic biocompatible and biodegradable hydrogels. *Bioact Mater*, 20: 53–63.

- <https://doi.org/10.1016/j.bioactmat.2022.05.020>
44. Danielson AP, Van-Kuren DB, Bornstein JP, *et al.*, 2018, Investigating the mechanism of horseradish peroxidase as a RAFT-initiator. *Polymers (Basel)*, 10: 741–755.
<https://doi.org/10.3390/polym10070741>
45. Nichol JW, Koshy ST, Bae H, *et al.*, 2010, Cell-laden microengineered gelatin methacrylate hydrogels. *Biomaterials*, 31: 5536–5544.
<https://doi.org/10.1016/j.biomaterials.2010.03.064>
46. Krishnamoorthy S, Noorani B, Xu C, 2019, Effects of encapsulated cells on the physical-mechanical properties and microstructure of gelatin methacrylate hydrogels. *Int J Mol Sci*, 20: 5061–5076.
<https://doi.org/10.3390/ijms20205061>
47. Gai HJ, Wu J, Wu CY, *et al.*, 2015, Synthesis and characterization of thermosensitive hydrogel with improved mechanical properties. *J Mater Res*, 30: 2400–2407.
<https://doi.org/10.1557/jmr.2015.233>